Quantitative evaluation of liver function by use of gadoxetate disodium (Gd-EOB-DTPA)-enhanced MR Imaging.

Akira Yamada, MD[1,2], Takeshi Hara, PhD[1], Feng Li, MD, PhD[1], Yasunari Fujinaga, MD, PhD[2], Kazuhiko Ueda, MD PhD[2], Masumi Kadoya, MD, PhD[2], and Kunio Doi, PhD[1]

[1] The University of Chicago, Department of Radiology, Chicago, USA

[2] Shinshu University School of Medicine, Department of Radiology, Matsumoto, Japan

Department of Radiology, Shinshu University School of Medicine, 3-1-1 Asahi, Matsumoto, Nagano 390-8621, JAPAN

Phone: 81-263-37-2650

Fax: 81-263-37-3087

E-mail: a_yamada@shinshu-u.ac.jp

Type of manuscript: Original research

Word count for the text: 2,926 words

Quantitative evaluation of liver function by use of gadoxetate disodium (Gd-EOB-DTPA)-enhanced MR Imaging.

Manuscript type: Original research

Advance in Knowledge:

The liver function corresponding to the plasma disappearance rate of indocyanine green (ICG-PDR) can be estimated quantitatively (R = 0.87) from the signal intensities and the volumes of the liver and the spleen on gadoxetate disodium-enhanced MR images.

Implications for Patient Care:

1. Our study results suggest that (Gd-EOB-DTPA)-enhanced MR imaging of the liver may improve the early detection and treatment of liver diseases by evaluating anatomic and functional information on the liver by one examination.
2. Gadoxetate disodium-enhanced MR imaging of the liver may allow quantitative estimation of segmental liver function.

Summary statement:

The liver function corresponding with ICG-PDR can be estimated quantitatively from the signal intensities and the volumes of the liver and spleen on gadoxetate disodium-enhanced MR images, which may improve the estimation of segmental liver reserve.

Abstract

Purpose: The purpose of this study was to determine if liver function correlating with indocyanine green (ICG) clearance could be estimated quantitatively from gadoxetate disodium-enhanced MR images.

Materials and Methods: This retrospective study was approved by the Institutional Review Board and the requirement for informed consent was waived. Twenty-three consecutive patients who had ICG clearance test and gadoxetate disodium-enhanced MR imaging with the same parameters as a preoperative examination were chosen. The 'Hepatocellular uptake index' (HUI) was determined by the equation $V_L(L_{20}/S_{20} - 1)$ from liver volume (V_L) and the mean signal intensity of whole liver (L_{20}) and whole spleen (S_{20}) on 3D-GRE T1-weighted images with fat suppression obtained at 20 min after gadoxetate disodium (0.025mmol/kg body weight) administration. The correlation of the plasma disappearance rate of indocyanine green (ICG-PDR) and various factors derived from MR imaging including HUI, iron/fat deposition in the liver/spleen, and the volume of the spleen (V_S) were evaluated by stepwise multiple regression analysis. The difference in future liver remnant ratio between HUI (rHUI/HUI) and volumetry (rV_L/V_L) was evaluated in 4 patients who had segmental heterogeneity of liver function.

Results: HUI and V_S were the factors significantly correlate with ICG-PDR (R = 0.87). The mean value and its 95% confidence interval for rHUI/HUI - rV_L/V_L were 0.18 (0.01 – 0.34).

Conclusion: The liver function correlating with ICG-PDR can be estimated quantitatively from the signal intensities and the volumes of the liver and spleen on gadoxetate disodium-enhanced MR images, which may improve the estimation of segmental liver function.

Introduction

Quantitative evaluation of liver function is important not only for monitoring of that function, but also for preoperative assessment of the liver reserve (1). The plasma disappearance rate of indocyanine green (ICG-PDR) has been regarded as a valuable tool for the quantitative assessment of liver function, because it is removed from the circulation exclusively by the liver (2). However, a reliable method for the quantitative anatomically based evaluation of liver function has not been established to date.

Gadoxetate disodium (Gd-EOB-DTPA; Primovist, Bayer Schering Pharma AG, Berlin) is a paramagnetic hepatobiliary contrast agent that can combine the features of extracellular agents with those of a hepatocellular contrast agent (3). The same transporting mechanisms, i.e., the organic anion transporter, are considered to be responsible for uptake of gadoxetate disodium and ICG in hepatocytes (4, 5); therefore, there is a possibility that gadoxetate disodium-enhanced MR imaging could be the basis of a useful method for quantitative evaluation of liver function similar to IGC clearance but with anatomic delineation of hepatic function, (6-11).

The purpose of this study was to determine if liver function corresponding to indocyanine green (ICG) clearance could be estimated quantitatively from gadoxetate disodium-enhanced MR images

Materials and Methods

Subjects

This retrospective study was approved by the Institutional Review Board of the Shinshu University and the University of Chicago, and the requirement for informed-consent was waived.

There were 59 consecutive patients (mean age ± SD = 69.9 ± 9.0, M:F ratio = 49:10) who had 3D-GRE T1-weighted gadoxetate disodium-enhanced MR imaging and an ICG clearance test as a preoperative evaluation within 4 weeks from June 2008 to December 2009 in the record at the Shinshu University Hospital. However, we selected only 23 patients for this study, as described below. Five patients (mean age, range = 73.6, 57-87, M:F ratio = 4:1) were excluded because pre-contrast MR imaging was not performed. Twenty-one patients (mean age, range = 68.9, 49-80, M:F ratio = 19:2) were excluded because the MR imaging parameters were different between pre and post-contrast enhanced MR imaging. Finally, 23 patients (mean age, range = 70.0, 41-84, M:F ratio = 17:6) were selected for the evaluation because they were the largest population in this study subjects whose MR imaging parameters (repetition time, TR / echo time, TE / flip angle, FA) were the same in pre and post-contrast enhanced 3D-GRE MR imaging There was no significant difference of the age and sex distribution between included and excluded patients. There were 6 patients without chronic hepatitis or liver cirrhosis, 6 patients with chronic hepatitis, and 11 patients with liver cirrhosis in this study group. No patient with renal dysfunction (serum creatinine > 2.0 mg/dL) was included in this study.

MR imaging

Imaging of the entire liver and spleen was performed prior to and 20 minutes after intravenous adminsitration of 0.025 mmol/kg of gadoxetate disodium by single-breath-hold 3D-GRE or with fat suppression (TR/TE/FA = 3.5 msec/1.42 msec/15 degree) on a MRI system (Trio Tim, Siemens, Germany) with 8 channels phased-array body coil and a parallel-imaging technique (the acceleration factor 2). Pre-contrast 2D-GRE T2*-weighted images (191-280 msec / 10 msec / 20 degree), pre-contrast 2D-dual-GRE T1-weighted images (106-165 msec / 1.23 and 2.46 msec / 80 degree) were also obtained to evaluate iron and fat

deposition in the liver and the spleen. The TEs in dual-GRE sequence were determined according to actual magnetic field strength of the MRI system (2.8 T).

Image analysis

Two radiologists (D.K. and M.M. who had 4 years and 3 years experience in diagnostic imaging, respectively. They were not included in authors.) independently drew the outlines of the liver and spleen on every slice of all MR images listed above in MR imaging section. In this procedure, MR images were presented on DICOM viewer (Osirix, Pixmeo, Geneva, Switzerland) and the outlines were drawn by free-hand contours (see Fig.1). The post contrast enhanced-3D-GRE images were always presented at first in order that observers can identify the liver parenchyma. The time limit for drawing outlines was not specified. In each patient, the volume of the liver and the spleen (V_L and V_S) on post contrast enhanced images and the mean signal intensity of the liver and the spleen at pre-contrast on T1-weighted images with fat suppression (L_0 and S_0), the mean signal intensity of the liver and the spleen at pre-contrast on in-phase T1-weighted images (L_{in} and S_{in}), the mean signal intensity of the liver and the spleen at pre-contrast on out-of-phase T1-weighted images (L_{out} and S_{out}), the mean signal intensity of the liver and the spleen at pre-contrast on T2*-weighted images (L_{T2*} and S_{T2*}) and the mean signal intensity of the liver and the spleen at pre-contrast at post-contrast on T1-weighted images with fat suppression (L_{20} and S_{20}) were obtained within the volume included in the outlines. The average values for all parameters (V_L, V_S, L_0, S_0, L_{in}, S_{in}, L_{out}, S_{out}, L_{T2*}, S_{T2*}, L_{20} and S_{20}) measured by the two radiologists were used for quantitative evaluation.

ICG clearance test

A dose of 0.5 mg/kg ICG was administered intravenously, and blood was withdrawn at 5, 10, and 15 min intervals following ICG administration. ICG-PDR was determined by regression analysis (12). ICG-PDR higher than 0.15 can be considered as normal liver function.

Feature values derived from gadoxetate disodium-enhanced MR images

We introduced the feature value $V_L(L_{20}/S_{20} - 1)$ which may be called the 'Hepatocellular Uptake Index' (HUI) as an index for the amount of gadoxetate disodium uptake into hepatocytes measured on gadoxetate disodium-enhanced MR imaging.

The feature value L_0/S_0, L_{T2*}/S_{T2*}, L_{out}/L_{in}, S_{out}/S_{in}, and V_S were evaluated to see the degree of the signal intensity difference between the liver and the spleen, the degree of the iron deposition difference between the liver and the spleen (13), the degree of fat deposition in the liver (14), the degree of fat deposition in the spleen (14), and the degree of splenomegaly due to portal hypertension, respectively.

The estimation of the segmental liver function in the patients with segmental heterogeneity of liver function

Conventionally, segmental liver function has been estimated by ICG clearance test and the volumetry (1). In this method, the segmental liver function could be estimated by the future liver remnant volume ratio (rV_L/V_L) multiplied by ICG-PDR based on the assumption that the liver function could be homogeneous; therefore, the ratio of the segmental liver function against to total liver function estimated by volumetry could be determined by rV_L/V_L. On the other hand, the segmental liver function could be estimated by the equation $rV_L(rL_{20}/S_{20} - 1)$ which may be called the 'Remnant Hepatocellular Uptake Index' (rHUI) as an index for the amount of gadoxetate disodium uptake into hepatocytes in remnant liver volume measured on

gadoxetate disodium-enhanced MR imaging taking into account of the heterogeneity of the liver function. Where rV_L is a remnant liver volume, rL_{20} and S_{20} are the signal intensity in the remnant liver and whole spleen. The future liver remnant function ratio could be described as rHUI/HUI by use of gadxetate disodium-enhanced MR imaging. We evaluated rV_L/V_L and rHUI/HUI in the patients with segmental heterogeneity of liver function due to known liver dysfunction such as portal vein embolization or obstructive jaundice affecting more than one liver subsegment. In this segmental analysis, two radiologists (D.K. and M.M.) drew the outlines of the non-affected liver on gadxetate disodium-enhanced MR imaging to obtain rV_L and rL_{20}. (see Fig. 2). The difference of two methods (rHUI/HUI - rV_L/V_L) was evaluated.

Statistical analysis

The mean value and its 95% confidence interval (CI) for the correlation coefficient between ICG-PDR and feature values (L_{20} and HUI) were determined by a bootstrap method with 2,000 bootstrap samples. The bootstrap sample size was determined according to the recommendation that the bootstrap sample size should be 1,000 or more to estimate CI (15).

The step wise multiple linear regression analysis of various feature values including HUI,, L_0/S_0, L_{T2*}/S_{T2*}, L_{out}/L_{in}, S_{out}/S_{in}, and V_S on ICG-PDR was done to evaluate the statistical significance of the various influences, such as iron and fat deposition and splnomegary, in the correlation between HUI and ICG-PDR. The entrance and exit tolerances for p-values of F-statistics were specified to 0.05 and 0.10, respectively.

The mean value and its 95% CI for rHUI/HUI - rV_L/V_L were evaluated to determine the statistical significance of the difference between HUI and volumetry in the estimation of segmental liver function.

All statistical analyses were carried out by use of MATLAB Version 7.11, R20010b (The MathWorks, Inc. Natick, MA, USA). No overlapping in 95% CI or p-value less than 0.05 were regarded to indicate significance.

Results

The liver characteristics of all patients obtained in this study are shown in Table 1.

The mean value and its 95% CI for correlation coefficients between ICG-PDR and feature values (L_{20} and HUI) were 0.634 (95% CI, 0.629 – 0.640) for L_{20} and 0.721 (95% CI, 0.717 – 0.726) for HUI (see Fig. 1, 3, 4).

The stepwise multiple linear regression analysis revealed that HUI and V_S were the factor significantly correlated with ICG-PDR in our study (Table 2). The regression coefficients and the R statistic for a multiple linear regression of HUI and V_S on ICG-PDR (ICG-PDR = $B_0 + B_1HUI + B_2V_S + e$) were $B_0 = 0.10$ (95%CI, 0.07 – 0.13), $B_1 = 0.12$ (0.08 – 0.15), $B_2 = -0.23$ (-0.34 – -0.11), and R = 0.87 (see Fig. 5).

The segmental heterogeneity of liver function affecting more than one liver segment was observed in 4 patients in our study. The liver characteristics of the patients are shown in Table 3. The mean value and its 95% CI for rHUI/HUI - rV_L/V_L were 0.18 (0.01 – 0.34).

Discussion

The feature value $V_L(L_{20}/S_{20} - 1)$ which may be called the 'Hepatocellular Uptake Index' (HUI) showed good correlation with ICG-PDR and the correlation was significantly higher than L_{20}. This result can be explained by two correction factors additional to the signal intensity of the liver on gadxetate disodium-enhanced MR imaging. One is the extracellular fluid (ECF) contrast enhancement effect of gadoxetate disodium in the liver approximated by

the signal intensity of the spleen (S_{20}) and the other is the inter-individual variation in the liver volume (V_L).

The local concentration of ICG and gadoxetate disodium taken up by hepatocytes decreases during the development of cirrhosis because of the decrease in hepatocytes and the increase in fibrous tissue (16). In addition,, the fibrosis of the liver results in a decrease in the incoming blood flow, and restriction of molecular movement within the extravascular space (17), which could be another possible cause of decreased uptake of ICG and gadoxetate disodium by hepatocytes. Although the cause of weak contrast enhancement of gadoxetate disodium in cirrhosis has not been fully clarified, the correlation between contrast enhancement of gadoxetate disodium and the degree of fibrosis has been observed in an animal model (18).

Gadoxetate disodium equilibrates rapidly between the intravascular and extravascular spaces according to the concentration gradient, following intravenous administration. Therefore the contrast enhancement effect of the gadxetate disodium is due not to uptake only in the hepatocytes but also it's presence in the ECF space (the sum of the intravascular and extravascular spaces) must be taken into account in the signal intensity of the liver on gadxetate disodium-enhanced MR imaging (L_{20}). After the gadxetate disodium reaches equilibrium state in ECF space (about two minutes after venous administration), the concentrations of gadoxetate disodium distributing in ECF spaces of the liver and the other organs fall in parallel as a result of renal and hepatic excretion. This phenomenon has been observed on MR imaging with use of gadoxetate disodium in extrahepatic organs such as the spleen (19). The distribution volume of gadoxetate disodium in the ECF correlates closely with the ECF volume after the equilibrium is reached, and the ECF volume is similar between the liver and spleen in normal liver and spleen (20). Therefore, the parameter $L_{20}/S_{20} - 1$

could serve as an index for the hepatocellular contrast enhancement effect corrected by the ECF contrast enhancement effect approximated by the signal intensity of the spleen.

The relation between the distribution volume and the degree of the liver fibrosis is controversial (21, 22). Van Beers et al reported that distribution volume of the liver would not be affected by the degree of liver fibrosis (21). In contrast, Hagiwara et al demonstrated significant increase in distribution volume between normal liver and liver fibrosis, however, the increase of distribution volume due to liver fibrosis comparing to normal liver has been reported as 10% (22). On the other hand, the relaxivity of gadoxetate disodium in ECF space (8.7 L/mmol) is about half comparing to that in hepatocytes (16.6 L/mmol), related to differences in micro viscosity (23). Therefore, the influence of various distribution volume in the liver according to liver fibrosis could be less than 10% and negligible in the signal intensity of the liver at 20 min after gadoxetate disodium administration (L_{20}).

On the other hand, our result showed that the volume of the spleen (V_S) could be a significant factor affecting the correlation between HUI and ICG-PDR. This can be explained by the effect of splenomegaly due to portal hypertension in splenic ECF volume. There have been several reports showing the hyperplasia of the red pulp and decrease of the vascular space density in the spleen during the development of splenomegaly due to portal hypertension (24). The increase of splenic hematocrit due to congestion may decrease the ECF space density in the spleen as has been suggested in the animal model with portal hypertension (25). Therefore, the decrease of ECF space density correlating with splenomegaly (increase in V_S) may lead the weak contrast enhancement of the spleen after the equilibrium point (decrease in S_{20}) and resulting in increase of HUI [$V_L(L_{20}/S_{20} - 1)$] on gadxetate disodium-enhanced MR imaging, however, this hypothesis must be confirmed by further investigation. In the future, more accurate index derived from HUI to estimate liver

function taking into account the volume of the spleen could be possible by use of gadxetate disodium-enhanced MR imaging.

If the parameter ($L_{20}/S_{20} - 1$) was analogous to the concentration of gadoxetate disodium taken up by hepatocytes, the total amount of gadoxetate disodium taken up by hepatocytes which can correlate with ICG-PDR would be found by the volume integration of $L_{20}/S_{20} - 1$. The similar idea has been proposed in the relation with histological evaluation of liver fibrosis. It was shown by Hashimoto et al. (26) that ICG-PDR was proportional to the total hepatic parenchymal cell volume, determined as the histologic parenchymal cell volume ratio multiplied by the liver volume obtained from computed tomography. The liver volume differs depending on not only the severity of chronic liver disease, but also on the physical constitution (27), and the total hepatic parenchymal cell volume differs individually. Thus, a correction for liver volume is necessary for estimation of ICG-PDR from the hepatobiliary contrast enhancement of gadoxetate disodium in the liver.

The signal intensity of the liver and the spleen in gadxetate disodium-enhanced MR imaging can be affected by various factors including liver function but also the difference of tissue specific relaxation time and the iron/fat deposition. However, our multiple regression analysis revealed that these effects were not significant in the correlation between HUI and ICG-PDR. This could be explained by the use of very short TE 3D-GRE sequence in the measurement of HUI in this study. The shorter TE is, the less T2*-weighted and the more T1-weighted image could be obtained. Thus, correlation of the contrast enhancement effect in the liver to liver function is much greater than to other factors affecting the signal intensity of the liver and the spleen in gadxetate disodium-enhanced MR imaging.

The uptake of ICG and gadoxetate disodium into hepatocytes reflects not only the hepatic cell function but also the hepatic blood flow (28); therefore the ICG-PDR and HUI might show discrepancy from the galactosyl-human serum albumin (GSA) scintigraphy

which is less affected by the hepatic blood flow, in some circulation disorders such as portosystemic shunts, the increased plasma volume, and the decreased cardiac output.

The liver volume and a quantitative liver function test such as the ICG clearance test have been reported to be significant predictors of postoperative liver failure and mortality (1, 29). However our result showed that the segmental liver reserve estimated by volumetry (rV_L/V_L) was significantly smaller than that estimated by HUI (rHUI/HUI). Therefore, volumetry could underestimate the segmental liver reserve because it could not take the heterogeneity of the liver function into account. Because the HUI can correlate with ICG-PDR very well and it can be determined directly from the volume and the signal intensity of a region of interest in the liver, the quantitative estimation of total and segmental liver function may be feasible. Therefore, gadoxetate disodium-enhanced MR imaging has the potential to provide the required information for the diagnosis and management of liver diseases by one examination, which can be essential to early detection and treatment.

Our study has several limitations. First, the study population was small, and further prospective validation with a large population especially on segmental variation in liver function is needed. Second, our eventual model did not use pre-contrast images; however, the effect of the difference in the pre-contrast signal intensity between the liver and the spleen was not significant. Therefore, HUI can be more convenient to apply for clinical practice than using signal intensity change between pre and post-enhanced images.

In conclusion, the **liver function corresponding with ICG-PDR can be estimated quantitatively from the signal intensities and the volumes of the liver and spleen on gadoxetate disodium-enhanced MR images, which may improve the estimation of segmental liver reserve.**

References

1. Seyama Y, Kokudo N. Assessment of liver function for safe hepatic resection. Hepatol Res. 2009; 39:107-16.
2. Sakka SG. Assessing liver function. Curr Opin Crit Care. 2007; 13:207-14.
3. Reimer P, Schneider G, Schima W. Hepatobiliary contrast agents for contrast-enhanced MRI of the liver: properties, clinical development and applications. Eur Radiol. 2004; 14:559-78.
4. Clement O, Muhler A, Vexler V, Berthezene Y, Brasch RC. Gadolinium-ethoxybenzyl-DTPA, a new liver-specific magnetic resonance contrast agent. Kinetic and enhancement patterns in normal and cholestatic rats. Invest Radiol. 1992; 27:612-9
5. Meier PJ, Eckhardt U, Schroeder A, Hagenbuch B, Stieger B. Substrate specificity of sinusoidal bile acid and organic anion uptake systems in rat and human liver. Hepatology. 1997; 26:1667-77.
6. Shimizu J, Dono K, Gotho M, et al. Evaluation of regional liver function by gadolinium-EOB-DTPA-enhanced MR imaging. Dig Dis Sci. 1999; 44:1330-7.
7. Schmitz SA, Muhler A, Wagner S, Wolf KJ. Functional hepatobiliary imaging with gadolinium-EOB-DTPA. A comparison of magnetic resonance imaging and 153gadolinium-EOB-DTPA scintigraphy in rats. Invest Radiol. 1996; 31:154-60.
8. Kim T, Murakami T, Hasuike Y, et al. Experimental hepatic dysfunction: evaluation by MRI with Gd-EOB-DTPA. J Magn Reson Imaging. 1997; 7:683-8.
9. Nilsson H, Nordell A, Vargas R, Douglas L, Jonas E, Blomqvist L. Assessment of hepatic extraction fraction and input relative blood flow using dynamic hepatocyte-specific contrast-enhanced MRI. J Magn Reson Imaging. 2009; 29:1323-31.
10. Ryeom HK, Kim SH, Kim JK, et al. Quantitative evaluation of liver function with MRI using Gd-EOB-DTPA. Korean J Radiol. 2004; 5:231-9.

11. Motosugi U, Ichikawa T, Tominaga L, et al. Delay before the hepatocyte phase of Gd-EOB-DTPA-enhanced MR imaging: Is it possible to shorten the examination time? Eur Radiol. 2009.

12. Moody FG, Rikkers LF, Aldrete JS. Estimation of the functional reserve of human liver. Ann Surg. 1974; 180:592-8.

13. Gandon Y, Olivié D, Guyader D, et al. Non-invasive assessment of hepatic iron stores by MRI. Lancet. 2004; 363:357-62.

14. Rinella ME, McCarthy R, Thakrar K, et al. Dual-echo, chemical shift gradient-echo magnetic resonance imaging to quantify hepatic steatosis: Implications for living liver donation. Liver Transpl. 2003; 9:851-6.

15. Martinez W, Martinez A. Bootstrap Methods. In: Computational statistics handbook with MATLAB. 2nd ed. London, Pa: Chapman & Hall/CRC, 2007; 256-262.

16. Malhi H, Gores GJ. Cellular and molecular mechanisms of liver injury. Gastroenterology. 2008; 134:1641-54.

17. Van Beers BE, Materne R, Annet L, et al. Capillarization of the sinusoids in liver fibrosis: non invasive assessment with contrast enhanced MRI in the rabit. Magn Reson Med. 2003; 49:692-9.

18. Tsuda N, Okada M, Murakami T. New proposal for the staging of nonalcoholic steatohepatitis: evaluation of liver fibrosis on Gd-EOB-DTPA-enhanced MRI. Eur J Radiol. 2010; 73: 137-42.

19. Runge VM. A comparison of two MR hepatobiliary gadolinium chelates: Gd-BOPTA and Gd-EOB-DTPA. J Comput Assist Tomogr. 1998; 22:643-50.

20. Kötz B, West C, Saleem A, et al. Blood flow and Vd(water): both biomarkers required for interpreting the effects of vascular targeting agents on tumor and normal tissue. Mol Cancer Ther. 2009; 8:303-9.

21. Van Beers BE, Leconte I, Materne R, et al. Hepatic perfusion parameters in chronic liver isease: dynamic CT measurements correlated with disease severtity. AJR Am J Roentgenol. 2001; 176:667-73..
22. Hagiwara M, Rusinek H, Lee VS, et al. Advanced liver fibrosis: diagnosis with 3D whole-liver perfusion MR imaging: initial experience. Radiology. 2008; 246:926-34.
23. Schuhmann-Giampieri G, Schmitt-Willich H, Press WR, et al. Precrinical evaluation of Gd-EOB-DPTA as a contrast agent in MR imaging of the hepatobiliary system. Radiology 1992; 183:59-64.
24. Cavalli G, Re G, Casali AM. Red pulp arterial terminals in congestive splenomegaly. A morphometric study. Pathol Res Pract. 1984; 178:590-4.
25. Kaufman S, Levasseur J. Effect of portal hypertension on splenic blood flow, intraplenic extravasation and systemic blood pressure. Am J Physiol Regul Integr Physiol. 2003; 284:1580-5.
26. Hashimoto M, Watanabe G. Hepatic parenchymal cell volume and the indocyanine green tolerance test. J Surg Res. 2000; 92:222-7.
27. Zhou XP, Lu T, Wei YG, Chen XZ. Liver volume variation in patients with virus-induced cirrhosis: findings on MDCT. AJR Am J Roentgenol. 2007; 189:153-9.
28. Nanashima A, Yamaguchi H, Shibasaki S, et al. Relationship between indocyanine green test and technetium-99m galactosyl serum albumin scintigraphy in patients scheduled for hepatectomy: Clinical evaluation and patient outcome. Hepatol Res. 2004; 28:184-190.
29. Suda K, Ohtsuka M, Ambiru S, et al. Risk factors of liver dysfunction after extended hepatic resection in biliary tract malignancies. Am J Surg. 2009; 197:752-8.

Tables

Table 1 Liver characteristics of the 23 patients.

Patients	Degree of LF	ICG-PDR [sec^{-1}]	HUI [L]	V_S [L]	L_{T2*}/S_{T2*}	L_0/S_0	L_{out}/L_{in}	S_{out}/S_{in}
#1	LC	0.064	0.425	0.403	0.643	1.434	1.008	0.915
#2	LC	0.071	0.239	0.157	0.736	1.040	0.868	0.939
#3	LC	0.072	0.270	0.115	0.654	1.123	1.035	0.946
#4	LC	0.082	0.203	0.079	1.073	1.068	0.975	0.978
#5	CH	0.083	0.588	0.296	0.712	1.304	0.987	0.898
#6	CH	0.105	0.419	0.136	0.839	1.221	0.859	0.905
#7	LC	0.121	0.365	0.194	0.810	1.102	0.996	0.936
#8	NL	0.122	0.787	0.292	1.028	1.229	1.010	0.972
#9	LC	0.130	1.046	0.413	0.631	1.125	0.991	0.911
#10	LC	0.134	0.451	0.122	0.732	1.143	1.003	0.841
#11	NL	0.135	0.961	0.150	0.684	1.137	0.957	0.912
#12	LC	0.149	1.165	0.324	0.624	1.632	1.018	0.930
#13	LC	0.149	0.721	0.125	0.560	1.434	0.882	0.902
#14	NL	0.152	0.930	0.043	0.769	1.215	1.018	0.926
#15	CH	0.153	0.515	0.148	0.690	1.214	0.967	0.887
#16	LC	0.158	0.464	0.156	0.820	1.167	0.953	0.913
#17	CH	0.179	0.698	0.089	0.840	1.151	0.978	0.888
#18	LC	0.181	0.874	0.099	0.788	1.376	0.981	0.915
#19	CH	0.182	0.407	0.102	1.163	1.108	0.963	0.957
#20	NL	0.193	1.296	0.274	0.785	1.286	0.992	0.957
#21	NL	0.207	1.068	0.139	0.890	1.040	1.013	0.898
#22	NL	0.215	1.001	0.077	0.984	1.464	0.977	0.872
#23	CH	0.267	1.475	0.108	0.836	1.049	0.960	0.913

LF = liver fibrosis, NL = normal liver, CH = chronic hepatitis, LC = liver cirrhosis, ICG-PDR = plasma disappearance rate of indocyanine green, HUI = Hepatocellular uptake index, V_S = volume of the spleen, L_{T2*}/S_{T2*} = signal intensity ratio of the liver to the spleen in T2*-weighted images, L_0/S_0 = signal intensity ratio of the liver to the spleen in pre-contrast enhancement T1-weighted images with fat suppression, L_{out}/L_{in} = signal intensity ratio of the liver in out-of-phase T1-weighted images to in in-phase T1-weighted images, S_{out}/S_{in} = signal intensity ratio of the spleen in out-of-phase T1-weighted images to in in-phase T1-weighted images.

Table 2 Stepwise multiple linear regression analysis of various factors on ICG-PDR.

Variables	Coefficients	p-value
HUI	0.116	< 0.01
V_S	-0.229	< 0.01
L_{T2*}/S_{T2*}	0.075	0.06
L_0/S_0	-0.016	0.69
L_{out}/L_{in}	-0.001	0.99
S_{out}/S_{in}	-0.152	0.42

HUI = Hepatocellular uptake index, V_S = volume of the spleen, L_{T2*}/S_{T2*} = signal intensity ratio of the liver to the spleen in T2*-weighted images, L_0/S_0 = signal intensity ratio of the liver to the spleen in pre-contrast enhancement T1-weighted images with fat suppression, L_{out}/L_{in} = signal intensity ratio of the liver in out-of-phase T1-weighted images to in in-phase T1-weighted images, S_{out}/S_{in} = signal intensity ratio of the spleen in out-of-phase T1-weighted images to in in-phase T1-weighted images.

Table 3 Characteristics of 4 patients with segmental heterogeneity of liver function

Patients	Affected segment	Cause	rHUI/HUI – rV_L/V_L
#4	S5, S6, S7, S8	OJ	0.428
#8	S8	OJ	0.120
#13	S5, S6, S7, S8	OJ	0.068
#22	S5, S6, S7, S8	PVE	0.083

OJ = obstructive jaundice, PVE = portal vein embolization, rHUI/HUI = HUI ratio of the unaffected liver to the total liver, rV_L/V_L = the volume ratio of the unaffected liver to the total liver.

Fig. 1 Axial 3D-GRE T1-weighted MR images with fat suppression (TR 3.5 msec/TE 1.42 msec/FA 15°) at 20 min after gadoxetate disodium administration obtained from a 64 years old female patient (#23) with metastatic liver tumor. The contrast between the liver and spleen is high on gadxetate disodium-enhanced MR image. The surounding liver was proven to be normal liver at surgical resection. HUI is high (1.068) consistent with high ICG-PDR (0.207). The outlines of the liver and the spleen are shown by green lines.

Fig. 2 Axial 3D-GRE T1-weighted MR images with fat suppression (TR 3.5 msec/TE 1.42 msec/FA 15°) at 20 min after gadoxetate disodium administration obtained from a 78 years old female patient (#22) with hilar bile duct carcinoma. Portal vein embolization (PVE) was performed in right branch of portal vein, and the signal intensity in the right hepatic lobe is decreased compared to that in the left hepatic lobe. The HUI ratio of the unaffected liver to total liver (rHUI/HUI) is 0.43, whereas the volume ratio of the unaffected liver to total liver (rV_L/V_L) is 0.32 and lower than rHUI/HUI. The outlines used to obtain rHUI and rV_L are shown by green lines.

Fig. 3 Axial 3D-GRE T1-weighted MR images with fat suppression (TR 3.5 msec/TE 1.42 msec/FA 15°) at 20 min after gadoxetate disodium administration obtained from a 73 years old male patient (#4) with hepatocellular carcinoma. The contrast between the liver and spleen is low on gadxetate disodium-enhanced MR image. The surrounding liver was proved to be cirrhotic at surgical resection. HUI was low (0.203) consistent with a low ICG-PDR (0.082).

Fig. 4 Correlation of HUI and ICG-PDR: The patients with splenomegaly (V_S > mean + 1SD) are indicated by a red circle. The patients without splenomegaly (V_S < mean + 1SD) are shown with blue circles. HUI: hepatocellular uptake index, ICG-PDR: plasma disappearance rate of indocyanine green, V_S = volume of the spleen, SD = standard deviation.

Fig. 5 Regression analysis of HUI and V_S on ICG-PDR: The patients with splenomegaly (Vs > mean + 1SD) are indicated by a red circle. The patients without splenomegaly (Vs < mean + 1SD) are shown with blue circles. HUI: hepatocellular uptake index, ICG-PDR: plasma disappearance rate of indocyanine green, V_S = volume of the spleen, SD = standard deviation.

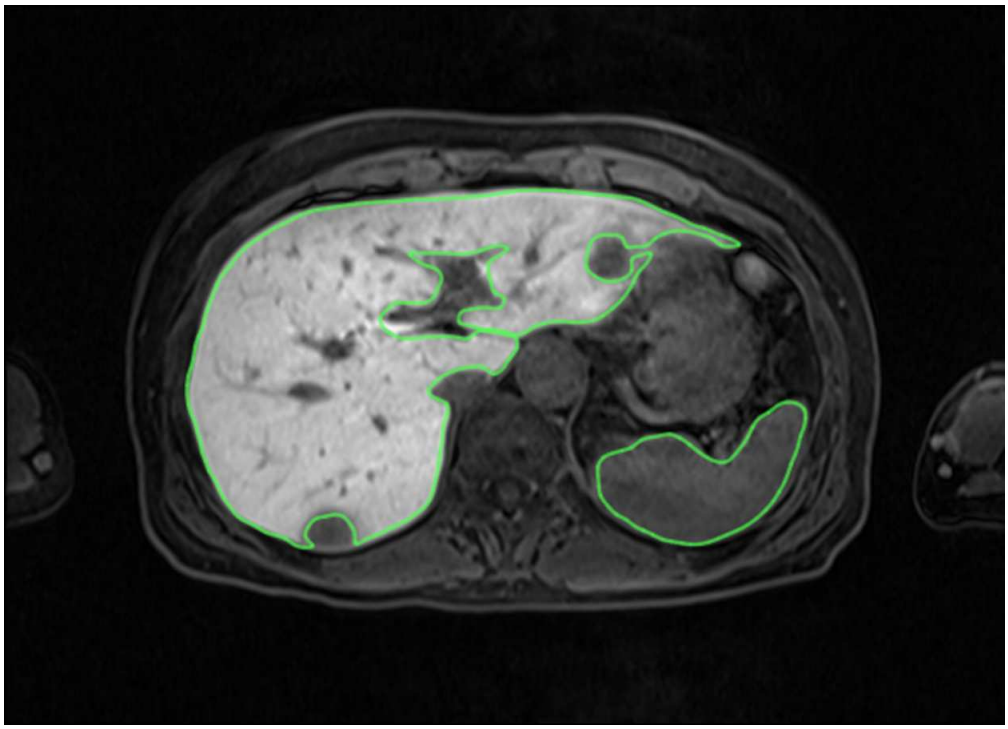

Figure 1. Case #23: A case with metastatic liver tumor: The contrast between the liver and spleen is high on gadxetate disodium-enhanced MR image. The background liver was proved to be normal liver by surgical resection. HUI is high (1.068) representing high ICG-PDR (0.207). The outlines of the liver and the spleen are shown by green lines.
106x76mm (300 x 300 DPI)

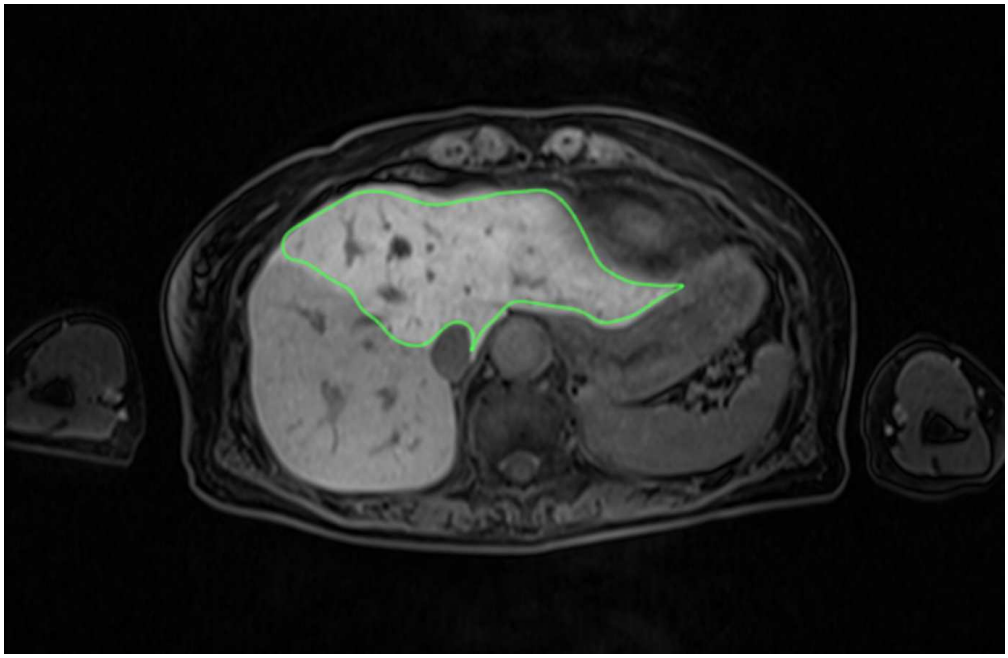

Figure 2. Case #22: A case with portal vein embolization (PVE): PVE was performed in right branch of portal vein, and the signal intensity in the right hepatic lobe is decreased compared to that in the left hepatic lobe. The HUI ratio of the unaffected liver to total liver (rHUI/HUI) is 0.43, whereas the volume ratio of the unaffected liver to total liver (rV_L/V_L) is 0.32 and lower than rHUI/HUI. The outlines to obtain rHUI and rV_L are shown by green lines.
117x76mm (300 x 300 DPI)

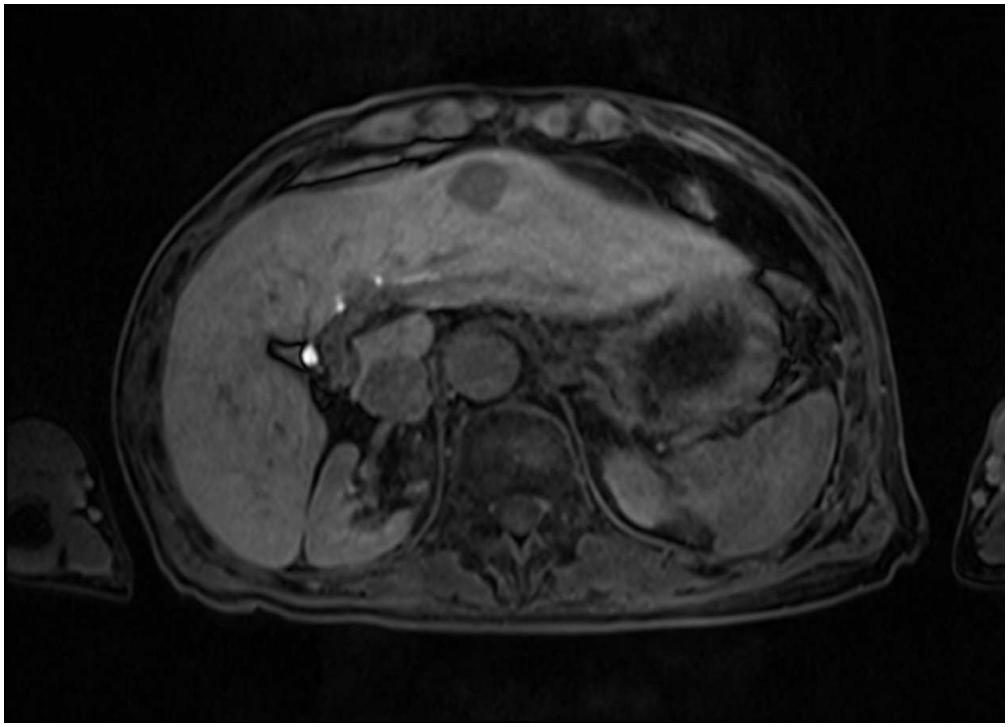

Figure 3. Case #4: A case with heparocellular carcinoma: The contrast between the liver and spleen is low on gadxetate disodium-enhanced MR image. The background liver was proved to be cirrhosis by surgical resection. HUI is low (0.203) representing low ICG-PDR (0.082).
106x76mm (300 x 300 DPI)

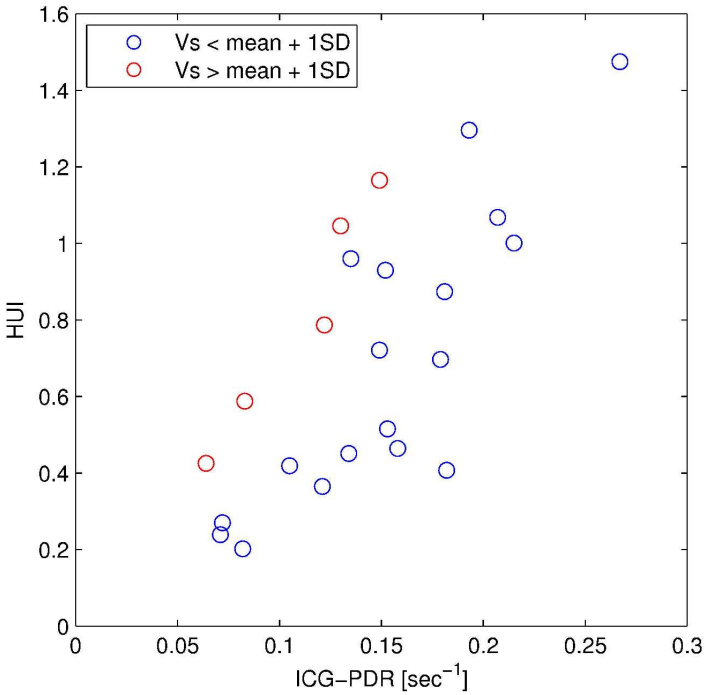

Figure 4. Illustration of correlation between HUI and ICG-PDR: The cases with splenomegaly (V_S > mean + 1SD) are shown by red circle. The cases without splenomegaly (V_S < mean + 1SD) are shown by blue circle. HUI: hepatocellular uptake index, ICG-PDR: plasma disappearance rate of indocyanine green, V_S = volume of the spleen.
158x118mm (600 x 600 DPI)

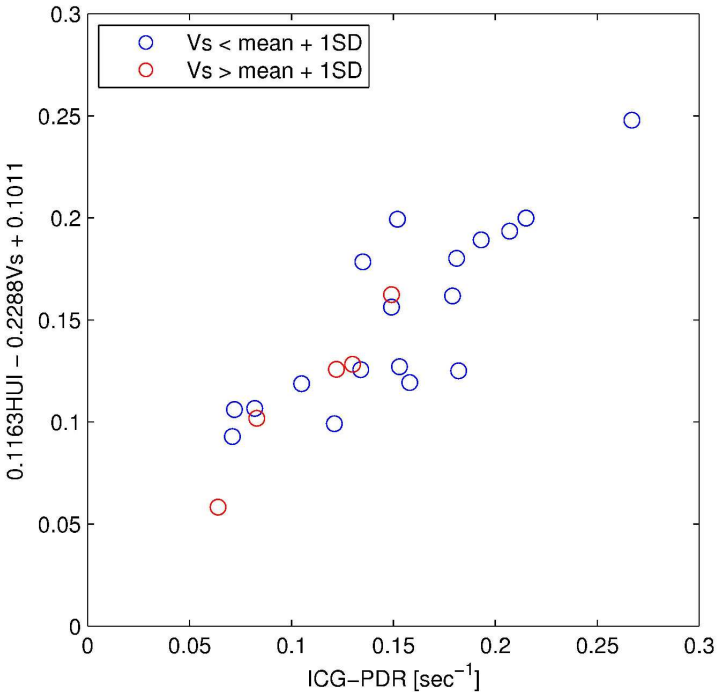

Figure 5. Regression analysis of HUI and VS on ICG-PDR: The cases with splenomegaly (V_S > mean + 1SD) are shown by red circle. The cases without splenomegaly (Vs < mean + 1SD) are shown by blue circle. HUI: hepatocellular uptake index, ICG-PDR: plasma disappearance rate of indocyanine green, V_S = volume of the spleen.
158x118mm (600 x 600 DPI)